8th International Symposium on Magnetic Bearing
August 26-28, 2002, Mito, Japan

FEEDBACK LINEARIZATION CONTROL OF AMB SYSTEM

Adam Piłat

University of Mining and Metallurgy, Department of Automatics,
Mickiewicza Av. 30, 30-059 Kraków, Poland,
ap@ia.agh.edu.pl

ABSTRACT

This paper presents the feedback linearization of the nonlinear AMB (Active Magnetic Bearing) system. The system contains bounded parameters and some nonlinearities. The full analysis of the feedback linearization is presented. For the linearized system LQ controller is designed. The real system experimental results for the tracking problem are presented.

INTRODUCTION

In recent years a number of rotary machineries using Active Magnetic Bearings were designed due to elimination of lubricant medium, vibration, noise, high velocities and loads. Most of those systems are controlled by DSP processors and classical PID control algorithm. A wide range of linear controllers was developed for AMB systems [6]. Some of nonlinear solutions were presented in [7], [8], [9]. The aim of this paper is to show that the exact linearization method improves control quality of the AMB system.

This paper continues author's research on magnetic levitation systems. Previous work had focused on one-dimension magnetic suspension system. A nonlinear control method was proposed [10]. The main conclusion about exact feedback linearization was that the method extends the stabilization area but suffers from high sensitivity on model mismatch.

In the case of AMB system there is also necessary to obtain a well identified mathematical model. The magnetic bearing system is characterized by nonlinearities coming from electromagnetic forces, state and control constraints and electrical characteristic of the power-supply actuator unit. Those strong nonlinearities causes that the linear model obtained by local linearization works well in a very small operating area around the operating point. If the operating point moves from the origin, the system can be unstable due to neglected nonlinearities (for example: tracking problem in the spindle application [5]).

What is new in this paper. First, the electromagnetic force is modeled using coil inductance as a function of the gap length. Next, the exact linearization method is applied to single axis of the AMB. Finally, the system is controlled from a standard PC computer, where the integrated real-time control and rapid prototyping environment is used.

System description

The AMB laboratory model [1] consists of the rotor suspended in two magnetic bearings. Each bearing is controlled in two perpendicular axes. The rotor position is measured by Bently Proximity sensors located in each axis. Electromagnet coils are controlled from power driver using PWM technique. Generally the system consist of 12 measurements (rotor positions and coil currents) and 8 control signals.

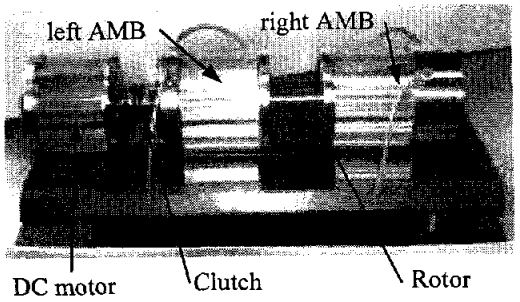

FIGURE 1: AMB - Laboratory model

Model of the AMB

The Active Magnetic Bearing consists of 4 electromagnets controlled separately. Electromagnets

are located in top and bottom of each axis. Figure 2 presents the configuration of the magnetic bearing and forces acting on the rotor.

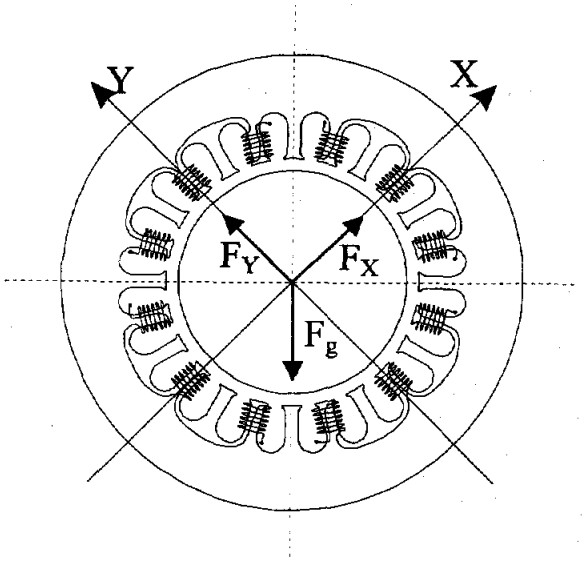

FIGURE 2: Configuration of the rotor in AMB

The electromagnetic force model is based on coil inductance (1).

$$\frac{dL(x_1)}{dx_1} = -\frac{L_0}{b} e^{\frac{-x_1}{b}} + 2cx_1 \qquad (1)$$

where:

L_0 coil inductance for rotor located at the electromagnet (distance equal to zero),

b, c constant values,

x_1 axial rotor position.

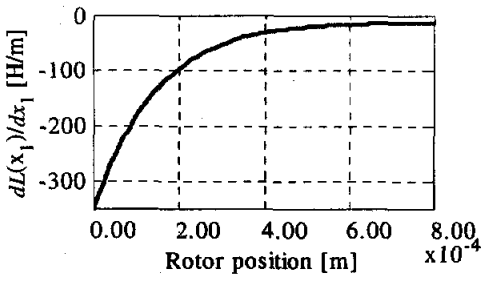

FIGURE 3: Coil inductance vs. rotor position

Electromagnetic force based on the proposed formula (1) gives better representation than standard one, due to electromagnet construction and air gap size. Forces generated by upper and lower electromagnet are given as follows:

$$F_{top} = \frac{1}{2} L^{(1)}(x_1) \cdot x_3^2 \,,\; F_{bottom} = \frac{1}{2} L^{(1)}(d - x_1) \cdot x_4^2$$

The electromechanical model of the single axis is given by (2). The control is differential.

$$\begin{aligned} \dot{x}_1 &= x_2 \\ \dot{x}_2 &= \frac{1}{2m}\left[L^{(1)}(x_1) \cdot x_3^2 - L^{(1)}(d - x_1) \cdot x_4^2\right] + \frac{F_{gV}}{m} \\ \dot{x}_3 &= \frac{a_3(u_{c3} - u) + b_3 - P1_3 x_3}{P2_3} \\ \dot{x}_4 &= \frac{a_4(u_{c4} + u) + b_4 - P1_4 x_4}{P2_4} \end{aligned} \qquad (2)$$

where:

x_1 axial mass position,

x_2 mass axial velocity,

x_3 current in upper coil of the considered control axis,

x_4 current in lower coil of the considered control axis,

u control signal – PWM duty,

u_{c3} constant control value,

u_{c4} constant control value,

m mass suspended in bearing,

d maximum air gap [m],

$F_{gV} = F_{gY}$ gravitation force acting in control axis,

$L(.)$ coil inductance,

a_i, b_i, $P1_i$, $P2_i$ actuator parameters $i = \{3,4\}$.

States and control signals are bounded as follows:

$x_1 \in [0, d]$, $x_2 \in \Re$, $x_3 \in [0,5]$, $x_4 \in [0,5]$,

$(u_{c3} - u) \in [0,1]$, $(u_{c4} + u) \in [0,1]$.

Constant control values depends on the current values chosen for the selected operating point. The selected values of the system parameters (Table 1) were obtained by identification procedures. The inductance parameters were obtained by optimization based on experimental results retrieved from system stabilization in the steady-state points.

TABLE 1: Parameters of AMB system

Parameter	Value	
m	0.00	[kg]
L_0	$5.2301 \cdot 10^{-2}$	[H]
b	$1.4897 \cdot 10^{-4}$	[m]
c	$-7.2187 \cdot 10^{3}$	[H/m^2]
d	$8.0 \cdot 10^{-4}$	[m]
a_3	8.44714	[A]
a	8.39955	[A]
b_3	1.56498	[A]

b_4	1.66871	[A]
Pl_3	0.802956	
Pl_4	0.799153	
$P2_3$	0.002512	[s]
$P2_4$	0.002322	[s]

For the operating point - rotor located in the bearing center – the electromagnetic force characteristic were calculated vs. rotor position and coil current. As shown in Figures 4 and 5 there is high sensitivity on force changes around the selected operating point.

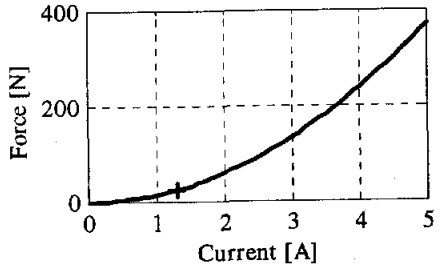

FIGURE 4: Force vs. current for fixed rotor position

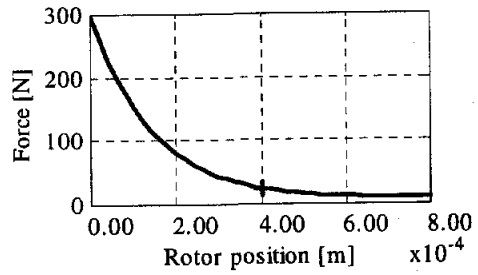

FIGURE 5: Force vs. rotor position for fixed current value

In this case standard local linearization can give satisfactionary results only in small area around operating point. Due to force changes the position and current stiffness are varying. In this case the idea of exact feedback linearization should be used to obtain linear system.

FEEDBACK LINEARIZATION

The aim of this method [2], [4] applied for the nonlinear model is to obtain linear system (see Fig. 6). The differential control strategy allows to treat each single axis of AMB as Single-Input Single Output (SISO) system.

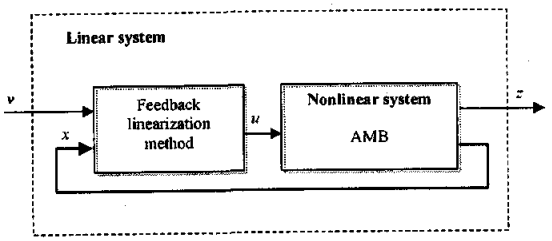

FIGURE 6: Feedback linearization method for AMB.

The local model of single axis of the AMB system can be described in general form:

$$\begin{aligned} \dot{x} &= f(x) + g(x)u \\ y &= h(x) \end{aligned} \tag{3}$$

where:

$$f(x) = \begin{bmatrix} x_2 \\ \frac{1}{2m_l} L^{(1)}(x_1)x_3^2 - \frac{1}{2m_l} L^{(1)}(d-x_1)x_4^2 + \frac{1}{m_l} F_{gx} \\ \frac{a_3 u_{c3} + b_3 - Pl_3 x_3}{P2_3} \\ \frac{a_4 u_{c4} + b_4 - Pl_4 x_4}{P2_4} \end{bmatrix}$$

$$g(x) = \begin{bmatrix} 0 \\ 0 \\ -\frac{a_3}{P2_3} \\ \frac{a_4}{P2_4} \end{bmatrix}, \quad h(x) = x_1 .$$

The calculated relative degree for the analyzed model is equal to 3. It means that the system contains internal dynamics. The control law decomposing the nonlinear system is described by:

$$u = \frac{1}{L_g L_f^2 h(x)} \left(v - L_f^3 h(x) \right) \tag{4}$$

where:

$$L_g L_f^2 h(x) = -\frac{x_3 L^{(1)}(x_1)}{m_l} \frac{a_3}{P2_3} - \frac{x_4 L^{(1)}(d-x_1)}{m_l} \frac{a_4}{P2_4}$$

$$\begin{aligned} L_f^3 h(x) = {} & \frac{x_2}{2m_l} \left[L^{(2)}(x_1)x_3^2 + L^{(2)}(d-x_1)x_4^2 \right] + \\ & + \frac{x_3 L^{(1)}(x_1)}{m_l} \frac{a_3 u_{c3} + b_3 - Pl_3 x_3}{P2_3} - \\ & - \frac{x_4 L^{(1)}(d-x_1)}{m_l} \frac{a_4 u_{c4} + b_4 - Pl_4 x_4}{P2_4} \end{aligned}$$

$$L_f = \frac{\partial h(x)}{\partial x} f(x),\ L_g = \frac{\partial h(x)}{\partial x} g(x),$$

are Lie derivatives of the function h across the vector fields f and g respectively.

New coordinates are given in the following form:

$$\begin{aligned} z_1 &= x_1 \\ z_2 &= x_2 \\ z_3 &= \frac{1}{2m_l} L^{(1)}(x_1) x_3^2 - \frac{1}{2m_l} L^{(1)}(d - x_1) x_4^2 + \frac{1}{m_l} F_{gV} \end{aligned} \tag{5}$$

Due to that relative degree value is less than nonlinear system size, it is necessary to find the coordinate z_4, to complete the transformation. Assuming that $L_g \phi_4(x) = 0$, the following partial differential equation should be solved:

$$\frac{\partial \phi_4(x)}{\partial x_3}\left(-\frac{a_3}{P2_3}\right) + \frac{\partial \phi_4(x)}{\partial x_4}\left(\frac{a_4}{P2_4}\right) = 0.$$

This can be done, assuming:

$$z_4 = \phi_4(x) = \frac{a_4}{P2_4} x_3 + \frac{a_3}{P2_3} x_4 \tag{6}$$

The Jakobian matrix of the transformation defined as:

$$J(\Phi(x)) = \begin{bmatrix} 1 & 0 & 0 & 0 \\ 0 & 1 & 0 & 0 \\ J_{3,1} & 0 & J_{3,3} & J_{3,4} \\ 0 & 0 & J_{4,3} & J_{4,4} \end{bmatrix},$$

is nonsingular for almost all x. The condition $J_{4,4} J_{3,3} \neq J_{4,3} J_{3,4}$ satisfies non singularity. That condition means e.g. that coils currents should have different values for the rotor located in the bearing center. In this case there exists global coordinates transformation from nonlinear system form to the linear one. The linear system dynamics is described by (7):

$$\begin{aligned} \dot{z}_1 &= z_2 \\ \dot{z}_2 &= z_3 \\ \dot{z}_3 &= v \\ \dot{z}_4 &= \frac{a_4}{P2_4} \frac{a_3 u_{c3} + b_3 - P1_3 x_3}{P2_3} + \frac{a_3}{P2_3} \frac{a_4 u_{c4} + b_4 - P1_4 x_4}{P2_4} \end{aligned} \tag{7}$$

Coordinates x_3 and x_4 can be obtained as a solution of the equations for z_3 and z_4 given in (5) and (6) respectively. As a result two possible solutions are given for each variable. Setting:

$$\alpha = \frac{1}{2m_l} L^{(1)}(x_1),\ \beta = -\frac{1}{2m_l} L^{(1)}(d - x_1),\ \chi = \frac{F_{gV}}{m_l},$$

$$\delta = \frac{a_3}{P2_3},\ \kappa = \frac{a_4}{P2_4},\ \rho = \alpha\kappa^2 + \beta\delta^2$$

the equations describing x_3 and x_4 coordinates as functions of z_3 i z_4 are given in the following form:

$$x_{3_1} = -\frac{\kappa\delta\left(-\delta^2\sqrt{\rho\chi - \rho z_3 + \alpha\beta z_4^2} + \beta\delta^2 z_4\right)}{\rho}$$

or

$$x_{3_2} = \frac{\kappa\delta\left(-\delta^2\sqrt{\rho\chi - \rho z_3 + \alpha\beta z_4^2} + \beta\delta^2 z_4\right)}{\rho},$$

$$x_{4_1} = \frac{\alpha\kappa z_4 - \delta^2\sqrt{\rho\chi - \rho z_3 + \alpha\beta z_4^2} + \beta\delta^2 z_4}{\rho}$$

or

$$x_{4_2} = \frac{\alpha\kappa z_4 + \delta^2\sqrt{\rho\chi - \rho z_3 + \alpha\beta z_4^2} + \beta\delta^2 z_4}{\rho}.$$

The result of analysis shows that only x_{3_1} and x_{4_1} satisfies states constraints. One can notice that for the analyzed system – single axis of AMB controlled differentially - it is possible to neglect the dynamics described by the fourth equation given in (7), because there is no influence on control and other system states. So, the linear system is obtained:

$$\begin{aligned} \dot{z}_1 &= z_2 \\ \dot{z}_2 &= z_3 \\ \dot{z}_3 &= v \end{aligned} \tag{8}$$

Due to existing state constraints of nonlinear system it is necessary to estimate constraints of the linear one (8). It can be done using simulation procedure. Constraints values for control v and state z_3 are presented in Table 2.

TABLE 2: Single axis parameters bounds

Parameter	Value
$z_{3\min}$	$-3.606 \cdot 10^{-13}$
$z_{3\max}$	$3.215 \cdot 10^{-13}$
$v_{\min}$	0.0
$v_{\max}$	$1.769 \cdot 10^{6}$

The state constraints for z_1 and z_2 are the same as for x_1 and x_2.

LQ Controller design

If the desired output of the linerized system (8) is given by $z_d = [z_{d1}, z_{d2}, z_{d3}]$, the error vector e can be defined as:

$$e = z_d - z .$$

A typical quadratic cost function has the form [3]:

$$J(v) = \frac{1}{2}\int_0^{\infty} [e^T(\tau)Qe(\tau) + v^T(\tau)Rv(\tau)]d\tau \qquad (9)$$

where:

Q is a non-negative definite matrix, $Q \geq 0, Q = Q^T$

R is a positive definite matrix, in this case R is a scalar.

It can be easily verified that the pair (A, B) of (8) is controllable. The LQ optimal control v^* is given by:

$$v^* = -K(z_d - z) \qquad (10)$$

where K is the feedback matrix.

The settings for the LQ controller were calculated numerically and next implemented to the simulation model and real system. One selection of the controller parameters is $Q = diag(1.2\cdot10^{15}, 1\cdot10^{6}, 1\cdot10^{6})$, $R = 1$, $K = [8.7702\cdot10^{-2} \quad 5.3518 \quad -1.2449\cdot10^{-1} \quad 1.8629\cdot10^{-2}]$

Controller parameters were calculated for the setected operating point $x = [4\cdot10^{-4} \quad 0 \quad 1.314 \quad 0]$.

REAL-TIME EXPERIMENTS

Real time experiment were performed in Windows 2000 environment using MATLAB/Simulink application with additional toolbox RTWT [11].

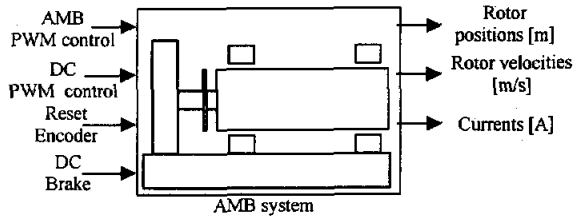

FIGURE 7: MATLAB/Simulink interface

The *AMB system* block presented in Figure 7 contains analogue input, encoder input and PWM output drivers to perform measurements and control. The AMB system was connected to the computer by the RT-DAC3 multi I/O board [12] equipped with XILINX programmable chip. User defined logic for the AMB system was applied. The simulation control loop scheme for a single axis is presented in Figure 8.

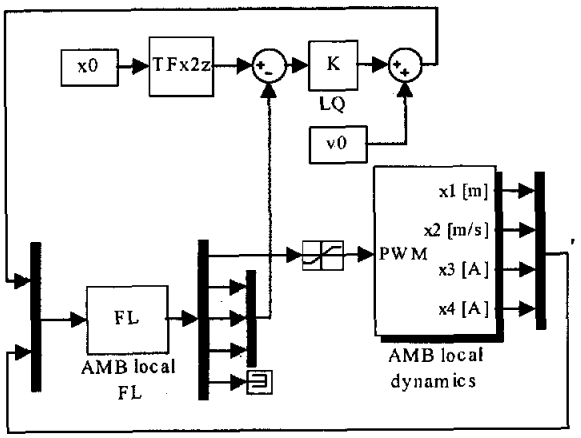

FIGURE 8: Control loop

The *TFx2z* block contains transformation from x to z coordinates. The *AMB local FL* block contains the control formula (4). For the real-time experiments the signals incoming and outgoing from the *AMB local dynamics* block were replaced by the *AMB system* block signals (see Figure 7). Real-time experiments were performed. The goal of the left bearing was to stabilize rotor position at the bearing center. In the right bearing desired rotor position was changed. First the square wave was set to obtain rotor movement in vertical direction. Rotor desired position was set $\pm 2.5\cdot10^{-4}$ m around the center. The result of the experiment is presented in Figure 9.

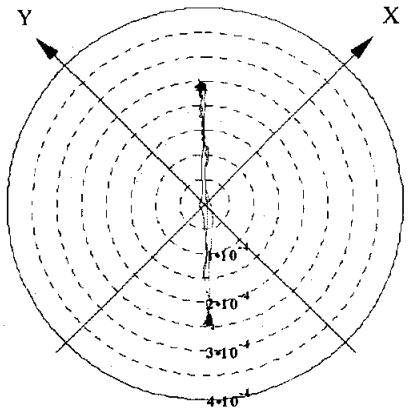

FIGURE 9: Right AMB – vertical rotor stabilization

Next, the shifted sine waves were applied to both axes, to obtain the circular trajectory of the rotor. The result

of this experiment is shown in Figure 10.

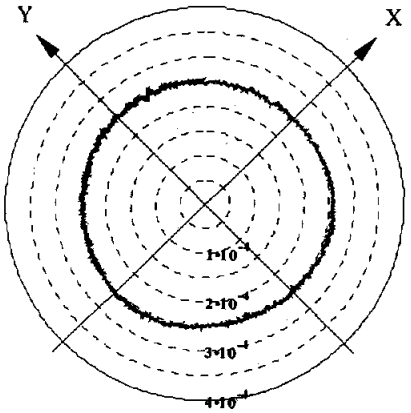

FIGURE 10: Right AMB – circular motion with radius equal to $2.5 \cdot 10^{-4}$ m

Finally the stabilization at the bearing center was applied. The rotational velocity was set to 550 rpm. The result of stabilization is presented in Figure 11.

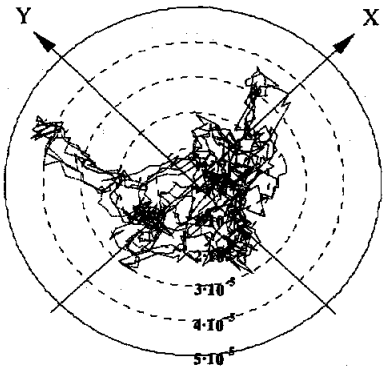

FIGURE 11: Right AMB – stabilization at 550rpm.

Notice that described model of the AMB doesn't take into consideration the rotational velocity of rotor. As shown above the feedback linearization method gives high stabilization zone and gives good results even the low stiffness is set (due to $x_4 = 0$). As an example of practical application of that control strategy can be in spindle machines. High stabilization range allows to minimize tool length. Another shape of the desired rotor movement can be easy adapted.

CONCLUSIONS

The feedback linearization gives the very high stabilization range of the rotor. With the LQ controller designed for the closed-loop AMB linearized system, the range of circular rotor movement was up to 500 micrometers. For the LQ designed for the system linearized in standard way the range of circular rotor movement was 30 micrometers. Feedback linearization method works successfully if model of the process is properly defined and all parameters are exactly identified. Process and model differences influence strongly on the control quality. For the laboratory Active Magnetic Bearing system used for this research, some parameters are difficult to identified e.g. inductance vs. rotor position.

REFERENCES

1. Dokumentacja techniczno-ruchowa stanowiska badawczego aktywnych łożysk magnetycznych. Instytut Maszyn Przepływowych, Politechnika Łódzka, Łódź, marzec 2001.
2. Isidori A.: Nonlinear Control Systems. 2nd Edition, Springer-Verlag 1989.
3. Kaczorek T.: Teoria sterowania i systemów, PWN Warszawa 1999.
4. Khail H. K.: Nonlinear Systems. Michigan State University, Prentice Hall, NJ 1993.
5. Kim M., Higuchi T., Mizuno T., Hara H.: Application of a Magnetic Bearing spindle to non-circular fine boring. 6th International Symposium on Magnetic Bearings, 5-7 August 1998, Massachusetts, USA, 22 ÷ 31.
6. Lee A., Fan Y.: Decentralized PID Control of Magnetic Bearings in Rotor System. 5th International Symposium on Magnetic Bearings, 28-30 August 1996, Kanazawa, Japan, 13 ÷ 18.
7. Lottin, J. Ponsart J., Mouille P.: Non linear control of Active Magnetic bearings. Digital implementation. 5th International Symposium on Magnetic Bearings, 28-30 August 1996, Kanazawa, Japan, 77 ÷ 82.
8. Lottin, J. Mouille P., Ponsart J.: Non linear control of Active Magnetic bearings. 4th International Symposium on Magnetic Bearings, 23-26 August 1994, Zurich, Switzerland, 101 ÷ 106.
9. Namerikawa T., Fujita M., Matsumura F.: Wide area stabilization of A Magnetic Bearing using exact linearization. 6th International Symposium on Magnetic Bearings, 5-7 August 1998, Massachusetts, USA, 733 ÷ 742.
10. Piłat A.: Feedback linearization and LQ control for magnetic levitation system. 6th International Conference on Methods and Models in Automation and Robotics, 28-31 August 2000, Międzyzdroje, Poland, 407 ÷ 412.
11. Real-Time Windows Target User's Guide. The Math Works Inc., Natick, ver. 1, USA, January 1999.
12. RT-DAC3, User's Guide. INTECO 2001, Poland.

This paper was supported by research grants of UMM and SCSR.